2010 IEEE International Conference on Robotics and Automation
Anchorage Convention District
May 3-8, 2010, Anchorage, Alaska, USA

Mini-quadrotor Attitude Control based on Hybrid Backstepping & Frenet-Serret Theory

J. Colorado, A. Barrientos, *Senior Member, IEEE*, A. Martinez, B. Lafaverges, and J. Valente

***Abstract*— This paper is about modeling and control of miniature quadrotors, with a special emphasis on attitude control. Mathematical models for simulation and nonlinear control approaches are introduced and subsequently applied to commercial aircraft: the *DraganFlyer* quadrotor, which has been hardware-modified in order to perform experimental autonomous flying. Hybrid Backstepping control and the Frenet-Serret theory is used for attitude stabilization, introducing a desired attitude angle acceleration function dependent on aircraft velocity. Finally, improvements on disturbance rejection and attitude tracking at moderate aircraft speeds are validated through various simulation scenarios (indoor navigation based on camera tracking), and flight experiments conducted on the DraganFlyer quadrotor.**

I. Introduction

Recent progress in sensor technology, data processing, and integrated actuators has made the development of Miniature Flying Robots –MFR fully possible [1]-[7]. The rotary-wing category (e.g. helicopters, quadrotor, coaxial) [4] draws attention to researchers because of their structural simplicity but the complexity on control. Depending of the size of the MRF, researches focus on different phenomena and new paradigms and challenges related to mechanical design, electronic miniaturization [4]-[6], and new approaches for gaining more autonomy [10]-[14].

In terms of control and autonomy navigation [10],[11], the *attitude control* of a mini-quadrotor is crucial. It provides the required stabilization to perform aggressive maneuvering and reliable navigation maintaining 3D orientation.

Classical control (e.g. PID) applied to attitude stabilization has being used for awhile, however, due to its design quadrotors are unable to move in an uncoupled way, and as a result of this under-actuation, standard control techniques do not work well on this craft [12]. On the other hand, most works [13]-[16] whether use non-linear control techniques to improve on the autonomous flight, but despite the substantial interest of studying dynamics nonlinearities, and design methodologies, little attention has been paid to the impact of aerodynamics effects [17] into the control scheme, which has a direct impact in the velocity and acceleration of the quadrotor. The influence of maneuvering while flying at moderate speeds has not been comprehensively explored.

For attitude control (at moderate/high aircraft speeds), advancing and retreating blades experience differing inflow velocities, resulting in a phenomenon called blade flapping. This induces roll and pitch moments at the blade root, and tips the thrust vector away from the horizontal plane which causes unsteady thrust behavior and poor attitude tracking.

To improve on the attitude control under these characteristics, this work focuses on applying a hybrid backstepping nonlinear control technique and the Frenet-Serret Theory–FST [18] (Backstepping+FST) that includes estimation of the desired angular acceleration (within the control law) as a function of the aircraft velocity during flight. In this sense, next section introduces the mathematical models used for simulation to finally test our control methodology into the DraganFlyer platform.

II. System Modeling

This section deals with the description of the fundamental concepts of the classic mechanics that are related to the rigid body dynamics modeling, presenting the Equations of Motion –EoM using the spatial operator algebra [19] applied to the quadrotor system: *The DraganFlyer* [20].

A. System Description

The DraganFlyer is a radio-controlled four-rotor aerial vehicle with four channels of input to control the motion in six Degrees-of-Freedom –DoF. Unlike a conventional helicopter where lift force generated by rotors can change direction by modifying the rotor roll/pitch angle, the motion of DraganFlyer can only be controlled by varying the speed of the four rotors, as the pitch angle of rotors is fixed. Those four propellers are in cross configuration, meaning that the two pair or propellers (1,3) and (2,4) turn in opposite directions (see Fig. 1).

Figure 1 shows the modified DraganFlyer platform. Xsens Inertial Measurement Unit –IMU, Bluetooth links, GPS, and additional electronics for distributing battery power have been incorporated within the system. Carbon fibers are also

Manuscript submitted February 2010. This work was supported by the Robotics and Cybernetics Group at Technique University of Madrid, Spain and funded under the project FRACTAL: Fleet of cooperative terrestrial and aerial robots, sponsored by the Spain Ministry of Education and Science (DPI 2006-03444) and ROBOCITY 2030 (S-0505/DPI/ 000235), http://www.robocity2030.org/

J. Colorado is a PhD student at the Technical University of Madrid, and researcher at the Robotics & Cybernetics Group at UPM, Spain. (e-mail: jcolorado@etsii.upm.es).

A. Barrientos, PhD, is a full tenure professor of the Technical University of Madrid, in Spain, and director of the Robotics & Cybernetics research group (e-mail: antonio.barrientos@upm.es).

B. Lafaverges is a graduated student at the INSA Lyon Institute in France.

A. Martinez and J. Valente are PhD students at the Technical University of Madrid, and researchers at the Robotics & Cybernetics Group at UPM, Spain.

use for holding the secondary mainframe (MF-2) structure where battery and IMU are placed.

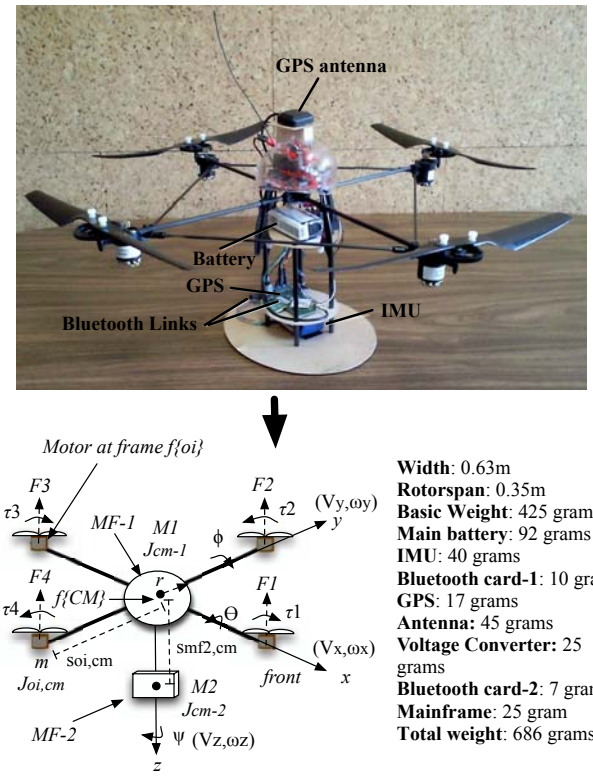

Width: 0.63m
Rotorspan: 0.35m
Basic Weight: 425 grams
Main battery: 92 grams
IMU: 40 grams
Bluetooth card-1: 10 grams
GPS: 17 grams
Antenna: 45 grams
Voltage Converter: 25 grams
Bluetooth card-2: 7 grams
Mainframe: 25 gram
Total weight: 686 grams

Fig. 1. **Above**: The DraganFlyer platform has been hardware-modified in order to address the required sensing and communication capabilities for achieving full autonomous navigation. **Below:** System description for modeling, including total weight from addressed components.

In terms of control, mapping the commands from control space to force space requires a model of the forces and their interactions. As shown in Fig.1 each motor produces a force F and torque (τ). For the rotational force-components, the rolling torque is produced by the forces of the right and left motors: τ2 and τ4 respectively and similarly, the pitching torque is produced by the forces of the front and back actuators: τ3 and τ1.

From a modeling perspective, the induced torques from the four rotors cancels through the airframe, placing considerable stress on it. This is a significant weakness of its design, and results in both distortion of the frame during flight and fixers coming loose due to the resultant vibrations. The small size, highly coupled dynamics, low air drag on the fuselage and high air drag on the rotors pose significant challenges in the control of this quadrotor.

B. *Dynamics Equations of Motion –EoM*

Assuming from Fig. 2 that O_i and CM are two points located on the rigid body, and $s_{oi,cm} \in \Re^3$ is the vector that joints both points, the translational and angular velocities (v,ω) and forces (f,τ) respectively at CM on the DraganFlyer in $\Re^3$ are related as shown in (1).

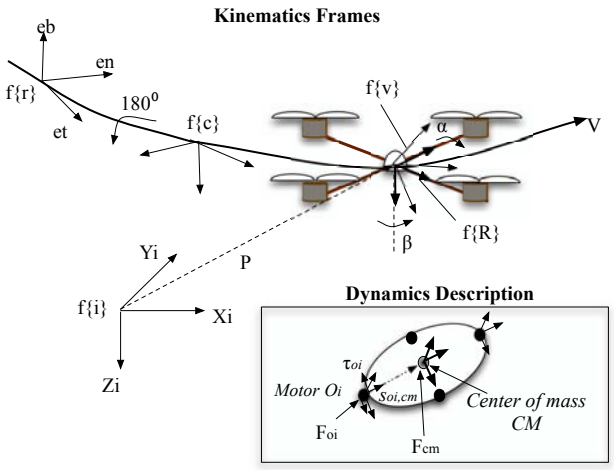

Fig. 2. MAV System Description for Modeling.

In terms of spatial algebra, the physical quantities are represented as 6x1 column vectors, in which Euler parameterization is used for kinematics transformation.

$$\dot{V}_{cm} = \begin{bmatrix} \dot{\omega}_{cm} \\ \dot{v}_{cm} \end{bmatrix} = I_{cm,T}^{-1}\left[F_{cm,T} - \dot{I}_{cm,T}V_{cm}\right] = \begin{bmatrix} J_{cm,T} - \tilde{s}_{oi,cm}m_T\tilde{s}_{oi,cm} & m_T\tilde{s}_{oi,cm} \\ -m_T\tilde{s}_{oi,cm} & m_T I \end{bmatrix}^{-1}\begin{bmatrix} \tau_{cm,T} - \tilde{\omega}_{cm}J_{cm,T}\tilde{\omega}_{cm} \\ f_{cm,T} \end{bmatrix} \quad (1)$$

The term $I_{cm,T} \in \Re^{6x6}$ is the mass operator that contains the inertia tensor operator $J_{cm,T} \in \Re^{3x3}$ of the vehicle due to rotors and electronics with total mass m_T. In addition, the term product $\dot{I}_{cm,T}V_{cm}$ refers to the spatial gyroscopic force acting on the vehicle's CM.

$$J_{cm,T} = \frac{2}{5}M_1 r^2 + M_2\left(\frac{a^2+b^2}{12} + s_{mf2,cm}^2\right) + m\left(r_m^2 + s_{oi,cm}^2\right) \quad (2)$$

In Fig 1 spherical-shape *–MF-1* is adopted from main electronics with mass M_1, whereas rectangular (M_2) and cylindrical (m, r_m) shapes for second electronics *–MF-2* (battery + IMU). The terms *(a,b)* refers to the lengths of the rectangular shape assumed for second electronics. The term $\tilde{s}_{oi,cm} \in \Re^{3x3}$ is the skew symmetric matrix corresponding to the vector cross product operator of $s_{oi,cm}$ (see Fig. 2), and finally $I \in \Re^{3x3}$ refers to the identity operator.

C. *Aerodynamics Forces and Airfoil Analysis.*

Although quadrotor vehicle dynamics is often assumed to be accurately modeled as linear for attitude control, this assumption is only reasonable at slow velocities. Even at moderate velocities, the impact of the aerodynamic effects resulting from variation in air speed is significant.

Lift and drag forces in (3) are dependent of the air density ρ_{air}, the rotor span area A, and proportional to the square of the propeller rotation speed Ω. Moreover a propeller

produces thrust by pushing air in a direction perpendicular to its plane of rotation. Whether the airflow is in the direction of the angular velocity vector or opposite depends on the shape of the propeller.

$$\begin{bmatrix} F_{lift} \\ F_{drag} \end{bmatrix} = \frac{1}{2}\begin{bmatrix} C_L \\ C_D \end{bmatrix} \rho_{air} A \Omega^2 \tag{3}$$

That propeller shape results on different lift C_L and drag C_D coefficient profiles, which are derived using a combination of momentum and blade theory [21]. Figure 3 shows some blade characteristics of the quadrotor's blades.

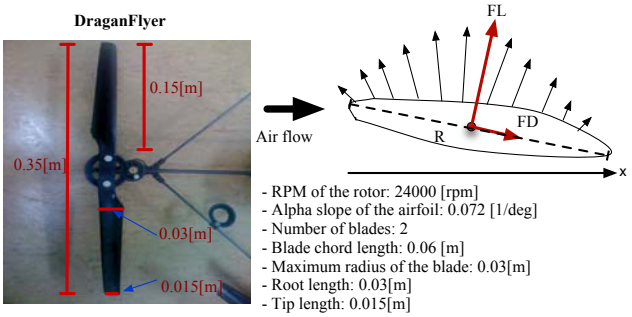

Fig. 3. DraganFlyer blade-description.

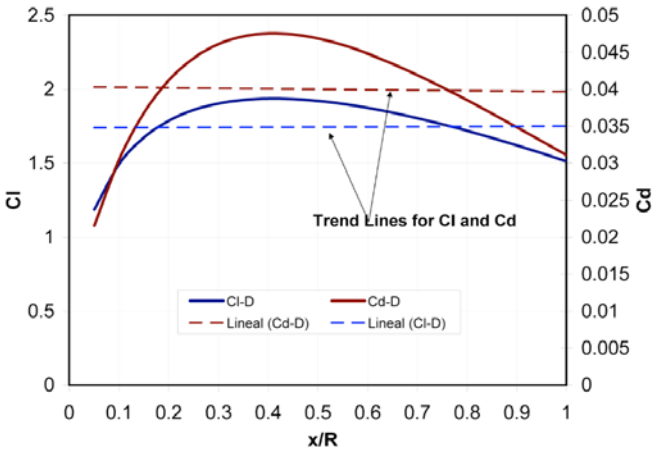

Fig. 4. Results for Blade Element Theory computation for lift C_L and drag C_D coefficients as a function of blade surface distance x/R.

In addition Fig. 4 shows the blade element theory numerical algorithm results for estimating both lift (C_L=2.07) and drag (C_D=0.035) coefficients based on blade parameters in Fig. 3.

$$\frac{\Omega(s)}{u(s)} = \frac{0.749}{0.116s + 1} \tag{4}$$

To address the aerodynamics effects from (3) into the equations of motion in (1) a model of the quadrotor's motors must be included using (4). The term $u(s)$ refers to the control command torque that achieves the motor rotation speed $\Omega(s)$. In addition, the following variables mapping must be considered:

$$\begin{aligned} F_{cm,T} &= \sum_{i=1}^{4} F_{lift,i} - F_{drag,i} \\ f_{cm,T,[x]} &= \tau_\phi = s_{i,cm}\left(F_4 - F_2\right) \\ f_{cm,T,[y]} &= \tau_\theta = s_{i,cm}\left(F_1 - F_3\right) \\ f_{cm,T,[z]} &= \tau_\psi = \tau_2 + \tau_4 - \tau_1 - \tau_3 \end{aligned} \tag{5}$$

From (5) the term $f_{cm,T,[x]}$ refers to the rotational *x-axis* force component, and the terms $F_i\left(\forall_i : i = 1..4\right)$ are the resultant lift force component of each motor.

III. Architecture for Autonomous Flight

For achieving full autonomous flight, two main modules compose the architecture for modeling and control: *The System Modeling* (previously introduced in section-II), and *The System control*.

As a first attempt, we tested on DraganFlyer a PID controller based on a simplified model. However, strong disturbances were poorly rejected. In the second attempt we reinforced the control using backstepping technique. This time, simulation and experimental results confirmed improvements in relation to disturbance rejection.

The backstepping technique has been used for some time for controlling quadrotors [22]-[24]. Improvements have been introduced thanks to combine integral action within the control law (integral-backstepping), which consequently asymptotic stability is guaranteed, as well as steady state errors cancelation due to integral action. Nonetheless, poor analysis has been conducted on specifically improving attitude control, while the aircraft is maneuvering at moderate speeds and performing aggressive changes in orientation. To improve on this, we have adopted the Frenet-Serret formulation used in vector calculus to describe the kinematic properties of the aircraft that moves along a continuous and differentiable curve in the Euclidian space. Consequently, improvements on attitude stabilization using integral-backstepping as a function of a desired aircraft acceleration command are achieved. Next section explains this issue in detail.

A. The Frenet-Serret Formulas

Figure 2 introduced the different frames used to operate the EoM. The Vehicle-frame f{v} and the Inertial-frame F{i} are related with each other *–in terms of Euler angles–* with a well known $R_{\{v\}}^{\{i\}}$ Euler matrix transformation. Two additional frames called the Frenet-frame f{r} and the rotated Frenet-frame f{c} are composed by three unit vector so-called the tanget (e_t), normal (e_n), and binormal (e_b), that move along the desired trajectory.

Imagine that an observer moves along the curve in time, using the attached frame at each point as its coordinate system. The angular momentum of the observer's coordinate system is proportional to the angular momentum of the frame, which is useful to extract the Euler reference angles

based on the manipulation of homogeneous transformations. To every point of the curve we can associate an orthonormal triad of vectors (a set of unit vectors that are mutually orthogonal) namely the tangent, the normal and the bio-normal (see Fig. 2). Properly arranging these vectors, we obtain a description of the curve orientation [18]. The unit vectors are then defined as:

$$e_t = \frac{\dot{P}}{V}, \quad e_b = \frac{\left(\dot{P}\times\ddot{P}\right)}{\left\|\dot{P}\times\ddot{P}\right\|}, \quad e_n = e_b \times e_t \tag{6}$$

Where the term $V = \left\|\dot{P}\right\| = \sqrt{\dot{P}_x^2 + \dot{P}_y^2 + \dot{P}_z^2}$. In the definition of a frame associated with the curve the original definition of the Frenet frame f{r} for counterclockwise rotating curves is used; in the case of a clockwise rotating curve, the *z−axis* of the Frenet frame f{r} points in the opposite direction upwards than the inertial frame f{i}. This new frame is called the rotated Frenet-frame f{c}. Now, we can express the coordinates of a vector given in the rotated Frenet Frame f{c} to the f{i} frame with the matrix:

$$R_{\{c\}}^{\{i\}} = R_x\left(180^\circ\right)\begin{bmatrix} e_t & e_n & e_b \end{bmatrix}^T \tag{7}$$

Note $R_x \in \Re^{3x3}$ refers to the standard rotation matrix about the *x-axis*. As far as the reference orientation $\left[\phi_R, \theta_R, \psi_R\right]^T$ of the body-fixed frame f{v} with respect to the inertial f{i} frame is concerned (the subscript *R* indicates a reference value), due to the dynamics, f{v} does not perfectly coincide with the f{c} frame. To eventually coincide with the reference desired frame f{R} (which is the real frame that provides the orientation consistent with the aircraft dynamics), the rotation of the f{v} frame from f{c} to f{R} can be expressed using customary aeronautical notation by considering the sideslip angle *β*, and the angle of attack *α* (see Fig. 2):

$$\beta = \sin^{-1}\left(\frac{\dot{P}_y}{V}\right), \quad \alpha = \tan^{-1}\left(\frac{\dot{P}_z}{\dot{P}_x}\right) \tag{8}$$

The overall rotation is composed by rotating about the *z-axis* through the angle *–β,* and then, about the *y-axis* through the angle *α*. Note in (9), $R_z, R_y \in \Re^{3x3}$ refer to the standard rotation matrixes about the *z-axis* and *y-axis* respectively.

$$\begin{aligned} R_{\{c\}}^{\{R\}} &= R_y^T(\alpha) R_z^T(-\beta) \\ R_{\{i\}}^{\{R\}} &= R_{\{c\}}^{\{R\}} R_{\{c\}}^{\{i\}\,T} \end{aligned} \tag{9}$$

Using the second derivative of $R_{\{i\}}^{\{R\}}$ with respect to time, the angular acceleration references are:

$$\begin{aligned} \ddot{\phi}^d &= \text{atan2}\left(\omega_{\{i\},23}^{\{R\}}, \omega_{\{i\},33}^{\{R\}}\right) \\ \ddot{\theta}^d &= \text{atan2}\left(-\omega_{\{i\},13}^{\{R\}}, \sqrt{\left(\omega_{\{i\},23}^{\{R\}}\right)^2 + \left(\omega_{\{i\},33}^{\{R\}}\right)^2}\right) \\ \ddot{\psi}^d &= \text{atan2}\left(\omega_{\{i\},12}^{\{R\}}, \omega_{\{i\},11}^{\{R\}}\right) \end{aligned} \tag{10}$$

For instance, the next step is to introduce the desired attitude accelerations in (10) within the attitude control using the backstepping methodology. Next section describes this process in detail.

B. Backstepping nonlinear control

The complete system control is composed by a cascade-connection of altitude, position and attitude controllers. However, attitude control is the heart of the control system, which maintains the mini-quadrotor stable and oriented towards the desired direction. This section shows *roll*-control derivation based on hybrid backstepping and the Frenet-Serret equations previously introduced. Note that for both *pitch* and *yaw*-control, the same methodology is used.

Attitude Control: Based on the dynamics model in (1), the first step is to consider the *roll* tracking error e_1, and its derivative with respect to time:

$$\begin{aligned} e_1 &= \phi^d - \phi \\ \dot{e}_1 &= \dot{\phi}^d - \omega_x \end{aligned} \tag{11}$$

A Lyapunov function (positive definite) is used for stabilizing the tracking error e_1 based on a virtual control law for setting the behavior of the angular speed ω_x:

$$V(e_1) = \frac{e_1^2}{2}, \quad \dot{V}(e_1) = e_1\left(\dot{\phi}^d - \omega_x\right) \tag{12}$$

The virtual control law for stabilizing the angular tracking error $e_2 = \omega_x^d - \omega_x$ is then defined as:

$$\omega_x^d = c_1 e_1 + \dot{\phi}^d + \lambda_1 \int e_1 \tag{13}$$

Replacing the ω_x^d term in (13), and deriving e_2 with respect to time:

$$\dot{e}_2 = c_1\left(\dot{\phi}^d - \omega_x\right) + \ddot{\phi}^d + \lambda_1 e_1 - \ddot{\phi} \tag{14}$$

Replacing $\dot{e}_1 = -c_1 e_1 - \lambda_1 \int e_1 + e_2$ into $\dot{e}_2$ in (14), and extracting from (1) the dynamics terms corresponding to $\ddot{\phi}$:

$$\begin{aligned} \dot{e}_2 = c_1\left(-c_1 e_1 - \lambda_1 \int e_1 + e_2\right) + \ddot{\phi}^d + \\ \lambda_1 e_1 - J_{x-cm,T}^{-1}\left[\dot{\theta}\dot{\psi}\left(J_{y-cm,T} - J_{z-cm,T}\right) + u_\phi\right] \end{aligned} \tag{15}$$

Solving u_ϕ in (15) using $\dot{e}_2 = -e_1 - \lambda_2 e_2$ for achieving *roll* stabilization:

$$u_\phi = J_{x-cm,T}\gamma_{FST} + \xi,$$
$$\gamma_{FST} = e_1\left(1 + c_1^2 - \lambda_1\right) + e_2\left(-c_1 - \lambda_2\right) + c_1\lambda_{11}\int e_1 - \ddot{\phi}^d, \quad (16)$$
$$\xi = \dot{\theta}\dot{\psi}\left(J_{y-cm,T} - J_{z-cm,T}\right)$$

Finally the term $\ddot{\phi}^d$ in (16) is replaced by the desired angular acceleration command obtained with the Ferret theory in (10). In order to validate that our assumption of improving disturbance rejection is indeed correct, Fig. 6 shows the experimental results for the first test performed. Control parameters are listed in Table I.

TABLE I
EXPERIMENT PARAMETERS DESCRIPTION

Symbol	Description	Value [Unit]
m_T	DraganFlyer Total weight	686 [gr]
$J_{cm,T}$	Inertial products [Ixx, Iyy, Izz]	[0.0075, 0.0075, 0.014] [Kg.m^2]
c_L, c_D	Lift and drag coefficients	[2.07, 0.035]
η_{IMU}	IMU noise parameter	0.004[rad/s]
c_1, c_2, λ_1	Backstepping+FST roll gains	[5.5, 0.5, 0.01]
c_3, c_4, λ_2	Backstepping+FST pitch gains	[10, 2, 0.01]
c_5, c_6, λ_3	Backstepping+FST yaw gains	[2, 1.5, 0.005]

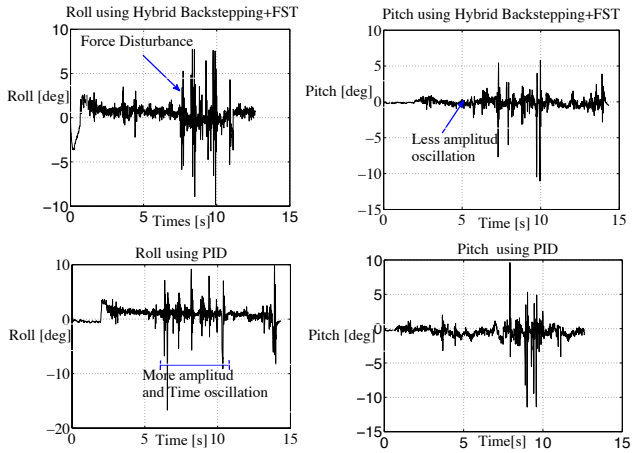

Fig. 5. (Experimental) Attitude control: Comparison between backstepping+FST control against PID controller while maintaining aircraft attitude angles to zero (hovering) despite disturbances addressed as shown in Fig. 6.

Note in Fig. 5 the PID controller proved to be well adapted to the quadrotor when flying near to hover. For this kind of test (hovering control), there are not huge differences of using the backstepping+FST control against single backstepping or either PID controllers. Note that just a slight difference in relation to amplitude and time oscillation is improved with the backstepping+FST. The reason is that this controller has been designed to improve on the attitude stabilization when aircraft is maneuvering.

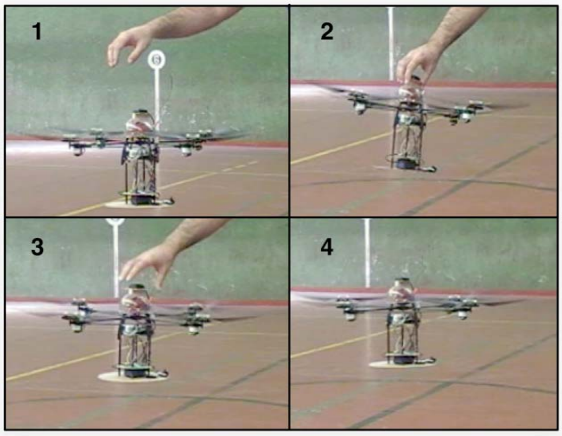

Fig. 6. Strong external disturbances addressed during experiment in Fig. 5. In addition, the controller has to deal with sensors noise and other non-desired and non-modeled effects.

To take advantage of this term, the trajectory of the aircraft must be smooth (i.e. three-times differentiable with respect to time) in order to achieve the desired values of attitude angles based on the references.

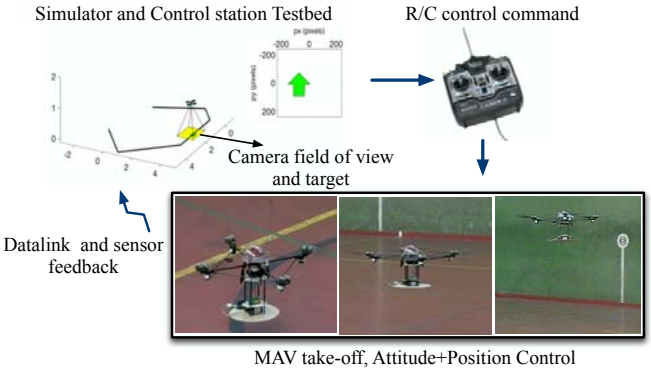

Fig. 7. Matlab-Testbed for testing full autonomous indoor navigation based on tracking a target on ground using vision.

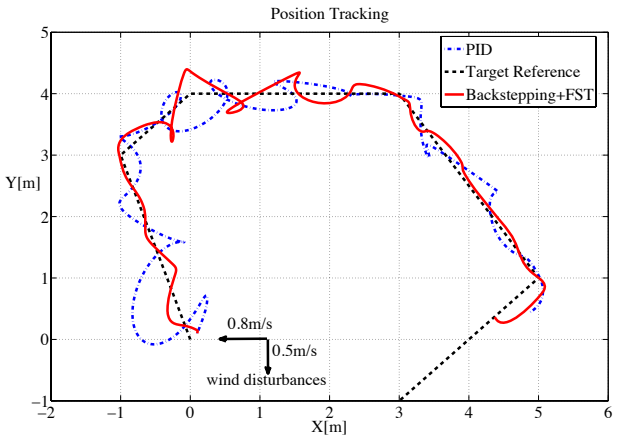

Fig. 8. (Simulation) X-Y Position Control while tracking target on ground at 2m/s. The advantage of using the hybrid Backstepping+FST for attitude control is significant for maintaining performance and reliability during Position tracking. The tracking error in position (despite external disturbances) is reduced (compared to PID control) thanks to the Backstepping+FST.

To achieve full indoor autonomous navigation, a camera must be placed on the quadrotor. For instance, the DraganFlyer platform has just been hardware-modified by addressing IMU and GPS for outdoor navigation. Our final goal on this project is to address the camera onboard in order to perform tracking tasks based on vision. Using a simulator developed on Matlab, we can test and tune the final concept to be developed (see Fig. 7).

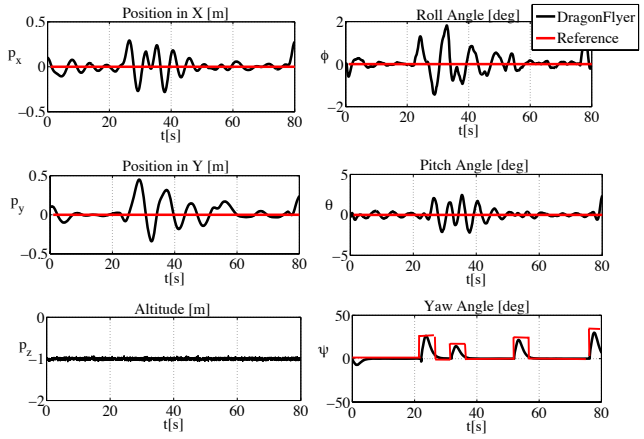

Fig. 9. Position+attitude control: Backstepping+FST maintains altitude over 1m above ground (negative due to frame reference in Fig. 2) while tracking the target at linear speed of 2m/s (green arrow in Fig. 8). Note positions are refer with respect to the vehicle's frame f{v}.

Figure 8 and 9 shows position control results. The mini-quadrotor perfectly tracks the target maintaining the orientation given by the target at 1m-altitude from ground and 2m/s target's speed.

IV. Conclusions

A backstepping+FST methodology has been proposed for attitude control. For full indoor navigation, future work includes addressing vision capability to the DraganFlyer, and finally testing position and altitude control beyond simulation. Nonetheless, results obtained in Fig. 8 are motivating. At high speed maneuvering (2m/s), the backstepping+FST's performance (in relation to error tracking) is about *2.5x* times better than using PID technique. The PID delays to reject the disturbance whereas the Backstepping+FST immediately compensates angular position based on velocity change rate, which consequently improves on the tracking error (in X-Y position). This improvement was basically achieved by introducing a desired angular acceleration command (as a function of the maneuvering velocity) that quickly responds to abrupt angular rate change, making the attitude stabilization more reliable.

References

[1] Zufferey, J.-C., Klaptocz, A., Beyeler, A., Nicoud, J.-D., and Dario. A 10-gram Microflyer for Vision-based Indoor Navigation. *Proceedings of the IEEE/RSJ International Conference on Intelligent Robots and Systems*, Beijing, China, 2006, p. 3267-3272.

[2] Wood, R. Design, fabrication, and analysis of a 3DOF, 3cm flapping-wing MAV. *Proceedings of the IEEE/RSJ International Conference on Intelligent Robots and Systems,* San Diego, CA, USA, 2007.

[3] Madangopal R., Khan Z., and Agrawal S. Biologically inspired design of small flapping wing air vehicles using four-bar mechanisms and quasi-steady aerodynamics. *Journal of Mech. Design*, vol. 127, pp. 809–816, July 2005.

[4] Nice, E. B., Design of a Four Rotor Hovering Vehicle, Master's thesis, Cornell University, 2004.

[5] Kroo I., Printz, F.B., *The Mesicopter: A meso-scale Flight Vehicle.* http://aero.stanford.edu/mesicopter/

[6] Karpelson, M., Gu-Yeon Wei, and Wood, R. A review of actuation and power electronics options for flapping-wing robotic insects. *The IEEE International Conference on Robotics and Automation,* Pasadena, CA, USA, 2008, pp. 779 - 786.

[7] Bouabdallah, S., Becker, M., and Siegwart, R. Autonomous miniature flying robots: coming soon!. *IEEE Robotics & Automation Magazine,* 2007, vol. 14 (3), 2007, p88 - 98.

[8] Bouabdallah, S., Siegwart, R, and Caprari, G., Design and Control of an Indoor Coaxial Helicopter. *Proceedings of the IEEE/RSJ International Conference on Intelligent Robots and Systems*, Beijing, China, 2006 pp. 2930 – 2935.

[9] Zufferey J-C., and Floreano D., Fly-inspired visual steering of an ultralight indoor aircraft, IEEE Transactions on Robotics, vol. 22, no. 1, pp. 137–146, 2006.

[10] Bouadi, H., Bouchoucha, M., & Tadjine, M. Sliding Mode Control based on Backstepping Approach for an UAV Type-Quadrotor. *Proceedings of world academy of science, engineering and technology,* Vol. 20, 2007.

[11] Waslander, S., and Hoffmann, G. Multi-Agent Quadrotor Testbed Control Design: Integral Sliding Mode vs. Reinforcement Learning. *The IEEE/RSJ International Conference on Intelligent Robots and Systems*, Alberta, Canada, 2005.

[12] Bouabdallah S., Noth A. PID vs LQ control techniques applied to an indoor micro quadrotor. *Proceedings of the IEEE/RSJ International Conference on Intelligent Robots and Systems*. Sendai, Japan, 2004.

[13] Olfati-Saber, R. Nonlinear Control of Underactuated Mechanical Systems with Application to Robotics and Aerospace Vehicles. *PhD thesis*, Massachusetts Institute of Technology, 2001.

[14] Bouabdallah, S., and Siegwart, R. Full Control of a Quadrotor. *Proceedings of the IEEE/RSJ International Conference on Intelligent Robots and Systems,* San Diego, CA, USA, 2007.

[15] Hoffmann, G., Rajnarayan, D. G., Waslander, S. L., Dostal, D., Jang, J. S., and Tomlin, C. J., "The Stanford Testbed of Autonomous Rotorcraft for Multi Agent Control (STARMAC). *Proceedings of the 23rd Digital Avionics Systems Conference*, Salt Lake City, UT, November 2004.

[16] Mokhtari, A. and Benallegue, A,. Dynamic Feedback Controller of Euler Angles and Wind parameters estimation for a Quadrotor Unmanned Aerial Vehicle. *Proceedings of the IEEE International Conference on Robotics and Automation*, New Orleans, LA, April 2004, pp. 2359–2366.

[17] Stepniewski, W. Z., Rotary-wing aerodynamics, Dover Publications, New York, NY, 1984.

[18] Hanson, A. Quaternion Frenet Frames: Making Optimal Tubes and Ribbons from Curves. Indiana University, *Technical Report*, 1-9, 2007

[19] Rodriguez G., Jain A., and Kreutz-Delgado K. Spatial operator algebra for manipulator modeling and control, *Int. Journal of Robotics Res*earch. 10(4) (1991), 371–381.

[20] The DraganFlyer. http://www.draganfly.com

[21] Wayne J. *Helicopter Theory*, Princeton University Press, Princeton, New Jersey, 1980.

[22] Bouabdallah S. and Siegwart R,. Backstepping and sliding-mode techniques applied to an indoor micro quadrotor. *Proceedings of the IEEE International Conference on Robotics and Automation,* Barcelona, Spain, 2005.

[23] Altug E., Ostrowski, J. P. and Mahony R. Control of a Quadrotor Helicopter Using Visual Feedback, *Proceedings of the IEEE International Conference on Robotics and Automation*, 2002.

[24] Erdinc Altu, James P. Ostrowski and Robert Mahony. Control of a Quadrotor Helicopter Using Visual Feedback. *Proceedings of the 2002 IEEE International Conference on Robotics and Automation*, Washington, DC USA, May 2004.